

# Low energy elastic electron scattering from ethylene

M A Khakoo, K Keane, C Campbell, N Guzman and K Hazlett

Department of Physics, California State University, Fullerton, CA 92831, USA

Received 2 June 2007, in final form 16 July 2007

Published 4 September 2007

Online at [stacks.iop.org/JPhysB/40/3601](http://stacks.iop.org/JPhysB/40/3601)

## Abstract

Normalized differential cross sections for elastic electron scattering from ethylene ( $\text{C}_2\text{H}_4$ ) are reported. The measurements are obtained using a novel version of the relative flow method with helium as the standard gas. Here, the relative flow method is applied without any prior knowledge of the gas kinetic molecular diameters of either the standard gas whose differential cross sections for electron scattering are known or the unknown gas whose differential cross sections for electron scattering need to be determined. Removal of this restriction is made possible by using an aperture-collimating source of the target gas instead of a conventional tube source. Importantly, the present method is accurate and more rapid than past elastic electron scattering experiments using the relative flow method, which employed tube-collimating gas sources. Our present measurements are used to test the reliability of past measurements for ethylene and so to resolve a recent disagreement between theory and experiment concerning the elastic electron scattering differential cross-section data for ethylene at low energy, by providing experimental values independent of any systematic errors that might arise when estimating gas kinetic molecular diameters for large polyatomics. Our new arrangement also extends the relative flow method to be applicable to gases whose gas kinetic molecular diameters may not be available, such as gaseous biomolecules.

## 1. Introduction

Low energy electron scattering from gaseous targets plays an important role in the physics and chemistry of plasmas. Quantitative measurements of differential elastic scattering of low energy electrons from atomic and molecular gases have, in the past, provided very useful tests of the electron scattering theory, as well as enabling calibration standards for the measurement of other differential scattering processes such as excitation, ionization and electron attachment [1] which play important roles in a range of processes in plasmas [2, 3], astrophysics [4] and in DNA break-up [5]. Elastic electron scattering remains a dominant process in the transport of low energy electrons through gaseous media and condensed matter, and is important in our understanding of the transport of electrons in various media such as organic tissue made

of biomolecules [6, 7], planetary atmospheres [4] and interstellar media, lasers and fusion plasmas [8].

Most measurements of elastic electron scattering differential cross sections (DCSs) for gaseous targets have been carried out using the relative flow method, which was initially applied to  $N_2$  by Srivastava *et al* [9]. This method is detailed in, e.g., Trajmar *et al* [10] and Brunger and Buckman [1] and involves a comparison of the electron scattering signal of the unknown gas X with that of He, whose DCSs are accurately known as a result of intense experimental and theoretical investigations (see, e.g., Nesbet [11] or Register *et al* [12]). However, the relative flow method is limited to targets whose gas kinetic cross sections are known or can be accurately estimated, and thus to atoms such as He and the noble gases, diatomic molecules such as  $H_2$ ,  $N_2$ ,  $O_2$ , CO and small polyatomic molecules such as  $CO_2$ ,  $CH_4$ ,  $C_2H_2$ ,  $C_2H_4$ , etc. It would therefore be useful if this method could be reliably extended to larger molecules whose gas kinetic molecular diameters are not available.

This paper concerns the implementation of the relative flow method without requiring any knowledge of the gas kinetic diameters for the molecular species being investigated. Our proposed method is a simple modification of the conventional relative flow method in which a collimating tube source is replaced by an aperture source. As a test of our aperture-based relative flow method, we have used He as our calibration standard and chosen two gases as test cases— $N_2$  whose DCSs are well known, and  $C_2H_4$  (ethylene) whose theoretical DCSs [13] are in some disagreement with experimental DCSs from two independent measurements [14] that are in excellent agreement with each other. Thus, the aim of our investigation is to investigate the following questions.

- (i) Can an aperture source perform reliably without applying the relative flow mean-free path condition using gas kinetic molecular diameters?
- (ii) If the answer to (i) is yes, can this setup help us to determine which of theory or experiment is correct for elastic scattering of electrons for  $C_2H_4$ ? If the theory were correct, it would imply that the relative flow method had systematic problems (such as wall-sticking or dimer formation) when extended to polyatomics with large gas kinetic molecular diameters.

## 2. The relative flow method with an aperture source

The most powerful, popular and successful method that has been used for measuring differential elastic electron scattering from relatively light atomic and molecular targets has been the relative flow method, which was first formulated by Srivastava *et al* [9] and has been applied extensively in the last 30 years to determine elastic electron scattering DCSs for these targets. The reader is referred to the extensive review of Brunger and Buckman [1] for an excellent summary of this work. In a differential electron scattering experiment, the scattered electron rate  $I_s(E_0, \theta)$  ( $s^{-1}$ ), at the incident energy  $E_0$  and scattering angle  $\theta$ , is given in terms of the incident electron fluence  $I_e$  ( $s^{-1}$ ) by the relation

$$I_s(E_0, \theta) = \int_{\tau} I_e n l \frac{d\sigma(E_0, \theta)}{d\Omega} \Delta\Omega, \quad (1)$$

where  $n$  is the target gas number density ( $cm^{-3}$ ),  $l$  is the effective path length of the electron beam through the gas,  $\frac{d\sigma(E_0, \theta)}{d\Omega}$  ( $= DCS(E_0, \theta)$ ) is the differential scattering cross section for the target gas atoms/molecules for the process under observation (elastic or inelastic scattering) for an (unpolarized) electron beam and  $\Delta\Omega$  is the solid angle subtended by the scattered electron detector at the collision region centre. Since all parameters on the right-hand side of equation (1) are dependent on the spatial displacement about the collision region centre

(which will be an extended region and not a point), the experimental value of  $I_s(E_0, \theta)$  depends on a convoluted volume integral of all these parameters about the collision region volume  $\tau$  (see, for example, Brinkmann and Trajmar [15]). Note that the number density of the gas,  $n$ , is related to the flow rate of gas  $\dot{N}$  by

$$\dot{N} = n A v, \quad (2)$$

where  $A$  is a nominal cross-sectional area of the target gas beam (perpendicular to the velocity  $v$ ,  $=KT/\sqrt{M}$ , from the kinetic theory of ideal gases,  $K$  is a constant and  $T$  is the absolute temperature of the gas); equation (2) can be inserted into equation (1) to obtain

$$I_s(E_0, \theta) = K' \int_{\tau} I_e \dot{N} \sqrt{M} (A^{-1} l) \frac{d\sigma(E_0, \theta)}{d\Omega} \Delta\Omega, \quad (3)$$

where  $K'$  is a constant that absorbs  $T$  and  $K$ . Note that equation (3) still remains a complicated integral over the collision region volume. The relative flow method takes advantage of a first-order factoring out of this integral when two gases are compared in equation (3), as will be discussed next.

In the relative flow method, using conventional electron scattering energy loss spectrometers, the gas (X) whose elastic DCS needs to be determined is compared to a standard gas under *identical* experimental conditions. The standard gas is usually He, whose DCSs are very accurately known from both theoretical [11] and experimental [12] standpoints. To achieve the required *identical* experimental conditions, the electron beam profile, the target gas profile and the scattered electron detector solid angle at the collision region (which together form a volume integral that relates the scattering signal to the differential cross section) should be the same [1, 10]. In general, by monitoring the electron current, leaving the collision region focusing properties of the electron gun section unchanged, and leaving the detection system unchanged, the identical collision region conditions are achievable for both He and X, if in addition the spatial profiles of the collimated target gases (He and X) are also the same. As was pointed out by Olander and Kruger [16], the profile of a gas beam emanating from a collimating tube structure depends primarily on the gas's collision mean-free path  $\lambda$  over a range of pressures behind the gas tube, even in the viscous flow regime. This mean-free path condition, producing identical angular gas beam distributions, was validated by recent work done in our group [17] for a range of atomic and molecular gases. Consequently, if any two gases are made to separately flow through the same collimating tube structure with identical  $\lambda$ 's, their profiles should remain identical. The mean-free path is given by

$$\lambda = \frac{1}{\sqrt{2} n \pi \delta^2}, \quad (4)$$

where  $n$  is the number density of the gas ( $\text{cm}^{-3}$ ) and  $\delta$  (cm) is its gas kinetic molecular diameter. The gas kinetic cross section ( $\text{cm}^2$ )  $\sigma$  is given by  $\pi \delta^2$  and the factor  $\sqrt{2}$  is a geometric factor arising from angle averaging of all possible hard-sphere scatterings between molecules in the gas phase. To obtain the same mean-free paths for the two gases He and X, the pressure behind the gas-collimating structure for helium ( $P_{\text{He}}$ ) and the gas X ( $P_{\text{X}}$ ) has to be in the ratio [1, 10]

$$\frac{P_{\text{He}}}{P_{\text{X}}} = \frac{\delta_{\text{X}}^2}{\delta_{\text{He}}^2}. \quad (5)$$

The  $\delta$ 's are determined from gas flow experiments which measure the viscosity of the gases under rarefied flow conditions. With the '*identical*' mean-free paths experimental condition met in equation (5), and from a consideration of equation (3) for both gases, the differential cross section for elastic scattering of gas X,  $\text{DCS}_{\text{X}}(E_0, \theta)$ , at the incident electron energy of

$E_0$  and scattering angle of  $\theta$  can then be determined from a simplification of equation (3), see [1, 10], as

$$\text{DCS}_X(E_0, \theta) = \text{DCS}_{\text{He}}(E_0, \theta) \frac{\text{RFR}_{\text{He}} I_{S_X}}{\text{RFR}_X I_{S_{\text{He}}}} \sqrt{\frac{M_{\text{He}}}{M_X}}, \quad (6)$$

where  $\text{DCS}_{\text{He}}(E_0, \theta)$  is the standard and well-known helium elastic scattering cross section, and  $I_{S_{\text{He}}}$  and  $I_{S_X}$  are, respectively, the subscripted electron scattering rates ( $\text{s}^{-1}$ ) for He and X, with  $\text{RFR}_{\text{He}}$  and  $\text{RFR}_X$  being the relative flow rates ( $\propto \dot{N}_{\text{He}}$  and  $\dot{N}_X$ , the flow rates for He and X, see section 3 for details) of atoms leaving the capillary tube ( $\text{s}^{-1}$ ) for He and X.  $M_{\text{He}}$  and  $M_X$  are the molecular masses of He and X, and it is assumed that the temperatures of both gases are the same. Expediently, we have used relative flow rates in equation (6). Equation (6) also assumes that the electron beam is the same for both He and X. In the general case that this is not exact, a (small) linear correction for electron current (provided that focusing of the electrons is not tampered with during the experiment) is adequate to correct for unequal electron currents for He and X, provided the current does not drift by more than  $\approx 10\%$ . Therefore,  $I_{S_{\text{He}}}$  and  $I_{S_X}$  are, respectively, the scattering rates from He and X (at the same  $E_0$  and  $\theta$ ) per unit incident electron current when a variation ( $< 10\%$ ) in the electron current is observed. The effect of variation in the electron current can be gauged on the reproducibility of the  $\text{DCS}_X(E_0, \theta)$  in the final analysis.

The present method, which bypasses the critical mean-free path condition in equation (5), is made possible by employing a thin collimating aperture for the gas source, instead of a conventional tube. For such a source, as long as the mean-free path of the gas remains much greater than the thickness of the aperture, the angular distribution of the gas should be constant, i.e., a cosine distribution convoluted with the aperture's extent [17, 18].

The motivation for the present work is to investigate the accuracy of the relative flow method (using conventional collimating tubes) for an important polyatomic target ( $\text{C}_2\text{H}_4$ , ethylene). This question arose when good qualitative agreement between the Schwinger variational calculations of Winstead and McKoy [13, 14, 19] and the experimental data of Panajotovic *et al* [14] was observed, but a somewhat consistent quantitative disagreement between the experimental DCSs and theory was found at intermediate incident energy ( $E_0$ ) values (20 and 30 eV), where theory was expected to be reasonably good. The experimental DCSs presented in Panajotovic *et al* [14] were a collaboration, with data taken independently at the Australian National University and Sophia University in Japan, and in most cases the agreement between the two independent experiments was excellent.

It was considered possible that a systematic error could have been introduced through the use of a hard sphere diameter of 4.94 Å for  $\text{C}_2\text{H}_4$  [14], which is an extended polyatomic, and that the application of the relative flow method using tube sources to larger polyatomic molecules warranted an independent experimental investigation. Although the results in [14] were taken at different source drive pressures to test the validity of the relative flow method in various mean-free path regimes, and an excellent agreement between experimental results for the different mean-free path regimes was obtained, it was nonetheless considered useful to apply an independent experimental method that requires no knowledge of molecular diameters for  $\text{C}_2\text{H}_4$  and He, to shed some light on this disagreement.

### 3. Method

The experimental apparatus (spectrometer, vacuum chamber, control equipment) has been detailed in previous papers, e.g., Khakoo *et al* [20], and only a brief description will be given here. Cylindrical electrostatic optics and double hemispherical energy selectors were utilized

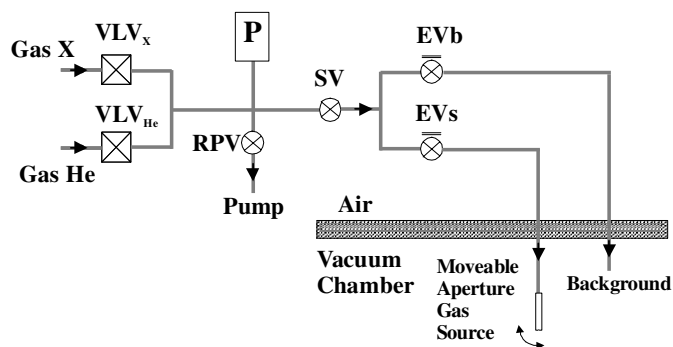


**Figure 1.** Schematic of our experimental gas handling system. Two-stage brass or steel diaphragm gas regulators, with Teflon tips, attached to the gas cylinder supplies were used to supply gas at 15–20 psi to the variable leak valves  $VLV_X$  and  $VLV_{He}$  (Granville Phillips<sup>TM</sup>, model 203) and subsequently into the feed line. RPV (Nupro<sup>TM</sup> Bellows SS-4HK) is the roughing pump valve and connects to a roughing pump for quick exhaust of gases especially from the cylinder side when the variable leak valves are opened wide and need to be pumped down; this was  $\approx 10$  mTorr in our system). SV (Nupro<sup>TM</sup> bellows SS-4HK) is a source isolation valve and isolates the vacuum chamber during roughing when PV is opened. EVb and EVs are electro-mechanical valves (ASCO<sup>TM</sup> H262VM) that feed the background (used also as a high vacuum exhaust of the gas line) and signal gas feed lines, respectively. P represents our ‘Baratron’ pressure manometer (MKS<sup>TM</sup> ‘Baratron’ model 221AHS-A-10). A 6.35 mm outer diameter refrigeration copper tubing is used throughout.

both in the electron gun and in the detector. Energy loss spectra of the elastic peak were collected at fixed  $E_0$  values and  $\theta$  by repetitive, multi-channel-scaling techniques. The target gas beam was formed by effusing the gas through an aperture which was constructed by mounting a thin disc of 0.025 mm thick brass shim stock into a flush recess at the end of a 6.35 mm o.d. and 4.3 mm i.d. brass tube as an aperture source. The aperture (0.3 mm diameter) was punched into the shim stock by a straight sharp sewing needle while the brass tube was rotating in the lathe, and thus the aperture was located centrally and flushed at the end of the tube. The tube was incorporated into a moveable source [21] arrangement. The moveable gas source method has already been well tested in our laboratory [22, 23] and determines background scattering rates expediently and accurately in electron scattering experiments. In this method, the collimating gas structure is moved into (signal + background) and out of (background) the collision region centre (see the appendix). Following the procedure detailed in [24] and employing the moveable gas source method:

- (i) We calibrated the behaviour of our gas-handling system (see figure 1) for He,  $N_2$  and  $C_2H_4$ , for the relative form of  $\dot{N}$  (the relative flow rate, RFR) versus the drive source pressure under steady state conditions for all three gases ( $P_s$ , see below). Here, one of the variable leak valves  $VLV_{He}$  or  $VLV_X$  appertaining to the gas of interest (respectively, He or X) was opened at a fixed setting, and the gas was allowed to flow through valves SV and EVs, with all other valves closed. The pressure  $P$  (measured at regular intervals with the ‘Baratron’ gauge, P in figure 1) was allowed to approach its steady state value  $P_s$ , and the  $P$  versus  $t$  data were fitted to an exponential form,  $P = P_s(1 - \exp(-a(t - t_0)))$ , where  $P_s$ ,  $a$  and  $t_0$  were fitted parameters [24, 25]. Figure 2(a) shows such a fit, which was used to determine the steady state value for  $P$  ( $= P_s$ ). Next, valve EVb was opened for a short time to bring the pressure  $P$  below the value of  $P_s$ , and then both EVb and EVs were closed. Now the gas filled a dead volume ( $V_0$ ) bounded by valves RPV, EVb, EVs and whichever of  $VLV_X$  or  $VLV_{He}$  was closed, with a source of gas filling it from

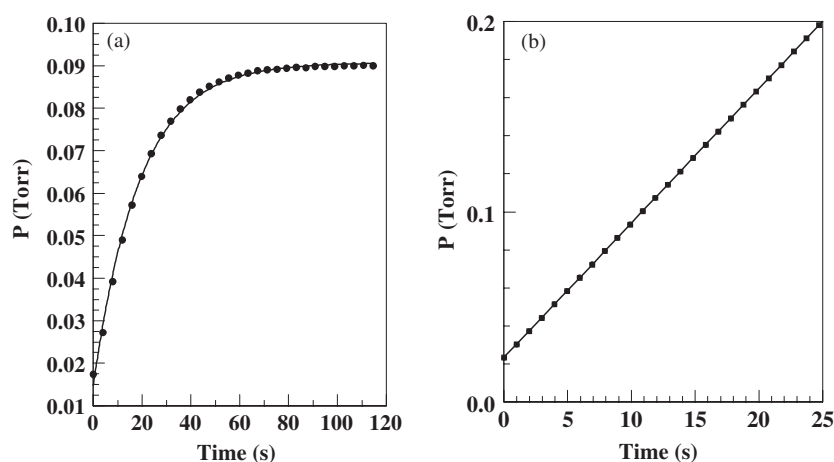


**Figure 2.** Graphs showing determination of (a) the source drive pressure  $P_s$  as an asymptote to the  $P$  versus  $t$  and (b) relative flow rate  $dP/dt$ , in our experiment, in this case for ethylene. See text for details.

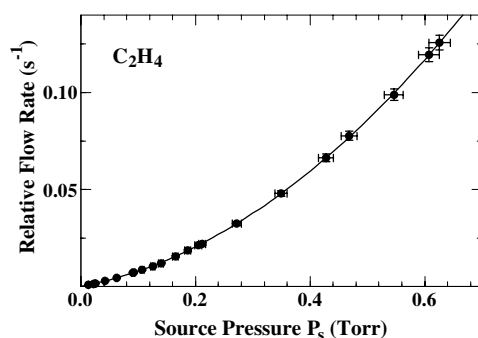


**Figure 3.** Source pressure versus relative flow rate,  $\propto \dot{N}$ , for the aperture source in the present work for  $C_2H_4$ . The nonlinearity is due to the finite conductance of the gas transport copper tubing from the manometer to the aperture.

whichever of  $VLV_X$  or  $VLV_{He}$  was open. From the ideal gas equation, the measured rate of change of  $P$  ( $dP/dt$ ) equals  $\dot{N}kT/V_0$ , i.e., proportional to the flow rate, with  $V_0$  being the fixed volume that is being filled by the gas. This  $dP/dt$  is the relative flow rate used in these measurements in equation (6). Figure 2(b) shows the linear rise of  $P$  versus  $t$ . Repeating this procedure for different settings of the variable leak valve, we were able to obtain a plot of  $dP/dt$  (=RFR) versus  $P_s$ . This plot conveniently enabled us to use the instantaneous ‘Baratron’ pressure to determine the instantaneous RFR for the gas. Figure 3 shows, for example, our determination of RFR versus  $P_s$  for  $C_2H_4$  for our experimental setup. The function used to analytically synthesize the dependence of RFR on  $P_s$  was a second-order polynomial in  $P$  which intersected the origin of  $P$  and RFR and could accurately reproduce the RFR to within 2%. This follows from the work of Sagara and Boesten [25] who showed that this dependence has physical significance at low  $P$  if described as

$$\text{RFR} = aP_s(1 + \varepsilon P_s). \quad (7)$$

**Table 1.** Gas flow parameters for the aperture source. See text for discussion.

Gas	$a$ (s Torr <sup>-1</sup> )	$\varepsilon$ (s Torr <sup>-1</sup> )	$\delta$ (cm)	$M$ (amu)	$a^*\sqrt{M}$	$e/\delta^2$
He	0.1551	0.7391	$2.18 \times 10^{-8}$	4.002	0.3102	$1.56 \times 10^{15}$
H <sub>2</sub>	0.2181	1.0500	$2.74 \times 10^{-8}$	2.016	0.3097	$1.40 \times 10^{15}$
N <sub>2</sub>	0.0596	2.1145	$3.75 \times 10^{-8}$	28.02	0.3157	$1.50 \times 10^{15}$
C <sub>2</sub> H <sub>4</sub>	0.0566	4.0705	$4.95 \times 10^{-8}$	28.03	0.2998	$1.66 \times 10^{15}$

In table 1, from our values of  $a$  and  $\varepsilon$  (for He, H<sub>2</sub>, N<sub>2</sub> and C<sub>2</sub>H<sub>4</sub>), it is clear that ‘ $a$ ’ is directly related to  $1/\sqrt{M_X}$  and describes the linear form which would be obtained at low  $P_s$  in the absence of gas–gas collisions in the tube connecting the pressure manometer to the aperture source. The presence of gas–gas collisions introduces nonlinear terms, of which the first has an additional dependence ( $\varepsilon$ ) to  $\delta^2$  (single collisions) related to the inverse mean-free path. In table 1, the ‘ $a$ ’ term is representative of collisionless flow within a standard deviation of 2%, whereas  $\varepsilon$  in the range of this work holds proportional to  $\delta^2$  to 7%, indicating a deviation at the high end of our  $\dot{N}$  versus  $P_s$  curves to  $P_s^2$  and that higher order terms were prevalent. Nevertheless, the second-order polynomial fit for  $P_s$  reproduces our flow rates to within the accuracy of our pressure manometer, i.e.,  $\pm 1.5\%$ .

- (ii) Next, we measured the intensity of the scattered electron signal at  $E_0 = 20$  eV and angle,  $\theta$ , of  $50^\circ$ , as a function of relative flow rate or  $dP/dt$ . We note here that the range of  $P_s$  used in our measurements for He, N<sub>2</sub> and C<sub>2</sub>H<sub>4</sub> did not exceed 1.2 Torr, 0.3 Torr and 0.2 Torr as measured at the ‘Baratron’ manometer, remaining well below the critical values of 5.3 Torr, 1.8 Torr and 1.0 Torr, respectively, where  $\lambda = t$  ( $t$  being the wall thickness of the aperture of 0.025 mm). We estimated from rough conductance considerations that the pressure measured at the ‘Baratron’ manometer was  $\approx 25\%$  higher than the pressure immediately behind the aperture. The scattered electron intensity was established for He, N<sub>2</sub> and C<sub>2</sub>H<sub>4</sub> to be linear within a conservative 3% errors, and is shown, for He and C<sub>2</sub>H<sub>4</sub>, in figure 4. This key result confirmed our hypothesis that the gas beam angular distribution did not factor into equation (6), and hence geometric terms remain constant (within the 3% error bars) as the flow rate is varied, i.e.,  $n \propto \dot{N}$  or the RFR. In measuring the scattered electron intensity, the gas beam was modulated into and out of the collision region for equal acquisition times. The scattered energy loss ( $E$ ) signal ( $E = -0.3$  eV to  $+0.3$  eV, in 100 channels) for the gas beam out of the collision region (background) was subtracted from the signal with the gas beam in the collision region (signal + background) to give the background-free signal. Details of the application of the moveable source method are described in [21], but are elaborated for the aperture source in the appendix. Importantly, this linear scattered electron signal versus relative flow rate signifies the experimental regime of pressure  $P_s$  for any gas of interest (here, He, N<sub>2</sub> or C<sub>2</sub>H<sub>4</sub>) that the experiment can be operated in with equation (6) remaining valid.
- (iii) We then carried out the standard relative flow electron scattering experiment putting in He and then X (X = N<sub>2</sub> or C<sub>2</sub>H<sub>4</sub>) and measuring elastic electron scattering intensities using the moveable source arrangement and applying equation (6) to determine the DCS for X, from the  $\dot{N}$  values of He and X, determined from  $\dot{N}$  versus  $P_s$  curves such as in figure 3. Thus, at every  $\theta$  at a fixed  $E_0$ , we measured the scattered electron rate (background corrected) for both He and X as well as the average electron current and the values of  $P_s$  behind the sources for both He and X, which were fed into equation (6) along with the DCS for He at the same  $E_0$  and  $\theta$  (from [11, 12]) to obtain a value of the DCS for X at this  $E_0$  and  $\theta$ . We note importantly here that we did not have to wait for  $P_s$  to reach any specific value (as would be required if we needed to satisfy equation (5)), so our measurements were



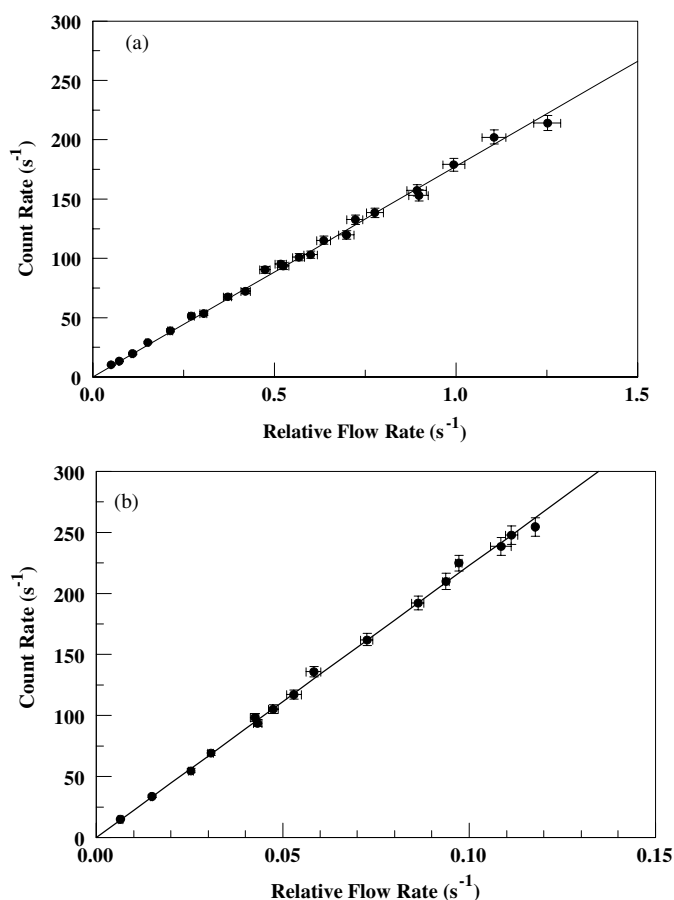


**Figure 4.** Scattered electron count rate (taken at  $E_0 = 20$  eV and  $\theta = 50^\circ$ ) versus RFR (for the aperture source) in the present work for (a) He and (b)  $\text{C}_2\text{H}_4$ . Pressure in the vacuum chamber for these flow rates ranged from  $3 \times 10^{-7}$  Torr to  $8 \times 10^{-6}$  Torr. Our base pressure is  $8 \times 10^{-8}$  Torr. Error bars ranged below 2%.

taken ‘on the fly’, i.e., as soon as  $P_s$  reached an equilibrium value set by the corresponding bleed valve  $\text{BV}_x$  or  $\text{BV}_{\text{He}}$ , with no connection to the ‘other’ gas through equation (5). This is a major advantage over conventional relative flow experiments, because to achieve the mean-free path condition posed in equation (5), as is required for conventional relative flow experiments with collimating tube structures, adjustment of the variable leak valves is generally challenging (these valves display significant back-lash when adjusted). Such experiments will meet equation (5) to within (generally) approximately 10% after some time spent in adjusting the variable leak valves. The present work provides a constant cosine distribution.

In our experiment, the sums of  $P_s$  and  $P_s^2$  were accumulated by the computer at the end every multi-channel energy loss scan of our elastic electron scattering peak (and used to determine the average  $P_s$  and its standard deviation for the data run). The average of  $P_s$  was found to change by less than 0.1% over any single data point. It was used to determine the RFR that was used in equation (6). We note here that to suppress secondary scattered electrons, the surfaces around the collision region were heavily sooted, included the gas aperture system.



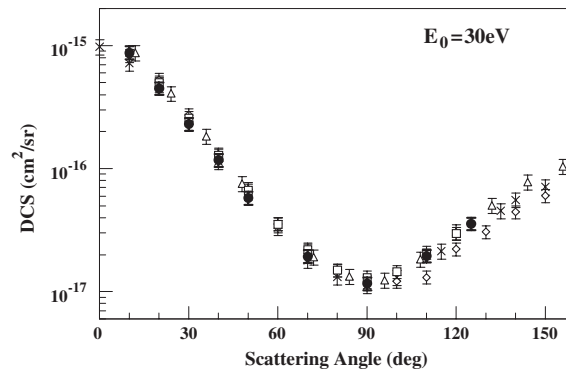


**Figure 5.** Normalized DCSs for elastic electron scattering from  $N_2$  at 30 eV: (●) present work, (×) Srivastava *et al* [9] renormalized by [10], (Δ) Shyn and Carignan [26], (□) Nickel *et al* [27] and (◇) Gote and Ehrhardt [28]. Average errors on present work are at  $\pm 12\%$ .

**Table 2.** Present DCS for elastic electron scattering from ethylene with errors (1 standard deviation). Units are in  $10^{-16} \text{ cm}^2 \text{ sr}^{-1}$ .

Angle (deg)	DCS 2 eV	Error	DCS 5 eV	Error	DCS 10 eV	Error	DCS 20 eV	Error	DCS 30 eV	Error
10			5.631	0.676	15.563	1.868	22.382	3.007	25.939	3.113
20	3.096	0.372	3.555	0.427	9.685	1.162	9.884	1.309	9.123	1.095
30	2.635	0.316	2.459	0.295	5.519	0.662	4.538	0.540	2.947	0.354
40	2.173	0.261	2.137	0.256	3.309	0.397	1.890	0.252	1.245	0.149
50	1.808	0.217	1.877	0.225	2.082	0.250	1.062	0.156	0.675	0.081
70	1.699	0.204	1.345	0.161	1.035	0.124	0.565	0.075	0.311	0.037
90	1.800	0.216	0.857	0.103	0.709	0.085	0.436	0.048	0.249	0.030
110	1.634	0.196	0.911	0.109	1.153	0.138	0.457	0.052	0.317	0.038
120							0.470	0.074		
125			1.025	0.123	1.302	0.156			0.363	0.044
130	1.342	0.161					0.557	0.069		

Also, the aperture was located 6 mm below the centre of the collision region to reduce its contribution of secondary electrons.

#### 4. Results

Our first (test of principle) experiments were on DCSs for  $N_2$  (which have been extensively measured). The DCSs for He (used as our test gas) were taken from [11, 12]. DCSs were measured at 20 eV and 30 eV, and we did not extend these to lower energies because of the observed excellent reproducibility of the DCSs and their agreement with existing measurements. Figure 5 shows, e.g., our DCSs for elastic scattering from  $N_2$  at 30 eV. Our DCSs have an upper error limit of 12% on average. We stress that no attempts were made in the process of acquiring data in the  $N_2$ /He experiments to work at any specific  $P_s$  for either of the gases to satisfy equation (5), but care was taken to stay well below the limit of  $\lambda \approx t$ . In light of the excellent agreement between our results and other experimental values for  $N_2$ , we proceeded to apply our method to  $C_2H_4$  and measured DCSs for elastic electron scattering, again using He as the test gas, at 2 eV, 5 eV, 10 eV, 20 eV and 30 eV. Our DCSs with respective error bars (which include reproducibility errors and statistical errors) are tabulated in table 2.

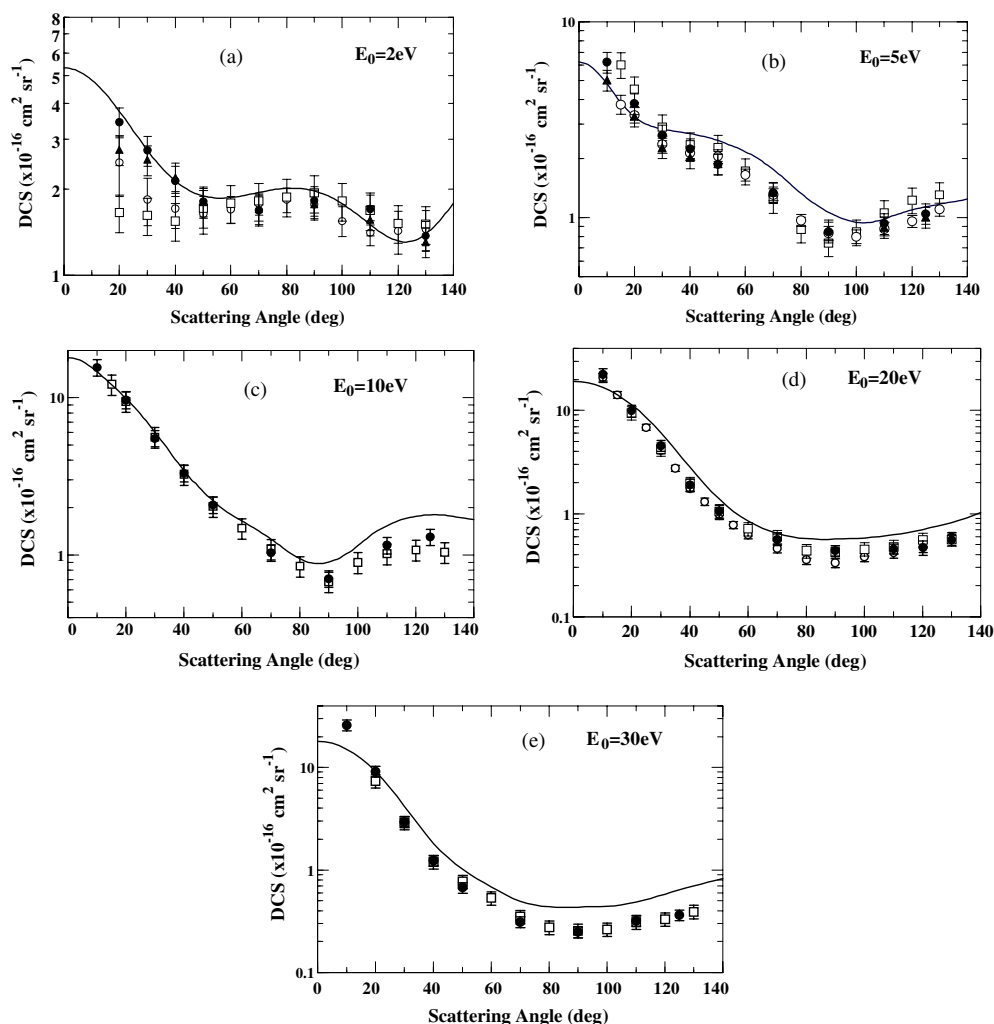


**Figure 6.** Normalized DCSs for elastic electron scattering from  $C_2H_4$  at  $E_0$  values indicated: (●) present work, (▲) present work taken over a week later with retuning of spectrometer, (○) ANU and (□) Sophia U in Panajotovic *et al* [14] and (—) theory, variational multi-channel Schwinger method of Winstead and McKoy [19], also published in [14].

Figures 6(a)–(e) show these DCSs compared to the recent work of Panajotovic *et al* [14]. Agreement with the previous experiments is excellent, except at 2 eV where our small-angle DCSs show better agreement with theory and with the ANU DCSs than with the Sophia U DCSs reported in [14]. Our small-angle DCSs have larger error bars, in the range of  $\pm 20\%$ . This is our lowest  $E_0$  and smallest  $\theta$ , where the collimation of the electron beam begins to be problematic and the background scattering becomes comparable to the signal at small  $\theta$ . We also note the excellent reproducibility of our DCSs at  $E_0 = 2 \text{ eV}$  and  $5 \text{ eV}$  comparing those taken at a later time on the experiment.

At 20 and 30 eV, our measurements clearly reaffirm the accuracy of experimental results of Panajotovic *et al* [14], despite initial concern about the possibility of systematic error that could arise from the value chosen for the molecular diameter. From these data, we conclude

that the source of disagreement lies in shortcomings of the theoretical calculations that have yet to be identified.

## 5. Conclusions

In conclusion, the present implementation of the relative flow technique with an aperture source, coupled with our moveable gas target method [11], has resulted in an altogether novel method which is very easy to apply, quick and does not depend on the adjustment of gas flow conditions to suit equation (5). It has been tested with both N<sub>2</sub> and more extensively with C<sub>2</sub>H<sub>4</sub> and has resulted in DCSs which are in excellent agreement with conventional experiments that used tube target-gas sources with employment of equation (5). The DCSs for C<sub>2</sub>H<sub>4</sub> are typical for a gas that is easily polarizable, showing predominantly forward scattering.

We note that at  $E_0 < 5$  eV, He is a very difficult test gas to use as a calibration standard at small  $\theta$  because the DCSs for elastic scattering from He (showing weak polarizability) are predominantly of a backward scattering nature. It would be useful to produce accurate elastic DCSs for a target such as N<sub>2</sub> at low energies. These DCSs are more forward peaked at small  $E_0$  values [1, 10], but they need to be more accurately determined for use as standards in low energy scattering experiments.

We also note that data can be acquired rapidly with the present method because of the advantage over the conventional relative flow method (using collimating tube structures) that equation (5) does not constrain the adjustment of the variable leak valves, thus reducing the time taken in going from gas X to He and back.

Further, and importantly, the present experimental method opens up the possibility of carrying out elastic scattering measurements on polyatomic targets whose  $\delta$  are not presently available, and which thus cannot be studied using the conventional relative flow method with collimating tube structures. This method can be used to, e.g., measure elastic electron scattering DCSs from exotic molecules such as biomolecules. Presently this method is being extended in our laboratory to measure low energy elastic scattering from alcohols, namely, CH<sub>3</sub>OH and C<sub>2</sub>H<sub>5</sub>OH, whose  $\delta$  values are not presently available and which are considered molecules of biological importance [29].

## Acknowledgments

This work was funded by grants from the National Science Foundation AMOP, Research in an Undergraduate Institution Program 0653450 and 0653452. We gratefully acknowledge the discussions with Drs B Vincent McKoy and Carl Winstead (Caltech, USA) who drew our attention to the disagreement between theory and experiment in electron C<sub>2</sub>H<sub>4</sub> scattering.

## Appendix. The moveable gas source method

In the moveable gas target source method [21], the collimated gas source is moved into and out of the collision region (⊙) as shown in figure A1. From figure A1, for a rotation angle  $\phi$  of the source, the emission angle  $\theta_g$  of the gas beam at the collision region can be derived as

$$\theta_g = \tan^{-1} \left[ \frac{\sin \phi / R}{(\cos \phi / R) - (1/R + r)} \right], \quad (\text{A.1})$$

where  $r$  is the closest distance of the nozzle tip from the collision centre and  $R$  is the radius of the arc of rotation of the nozzle tip. From these considerations, the relative beam intensity

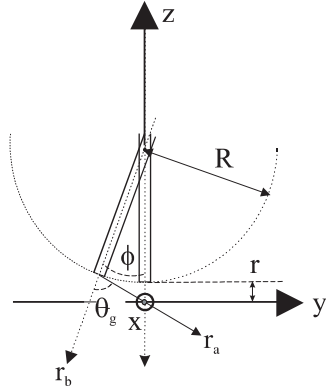


**Figure A1.** Diagram of the moveable target source with an aperture. See text for definitions and discussion.

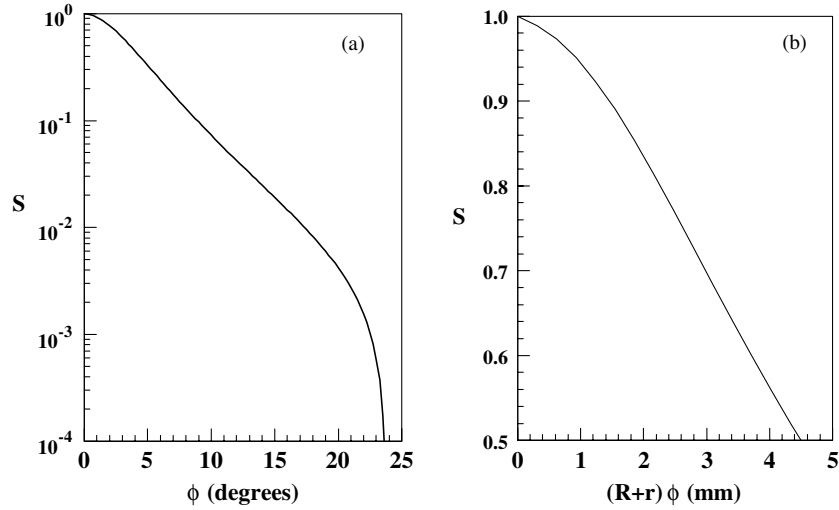


**Figure A2.** The relative gas beam intensity  $S$  (equation (A.2)) for the moveable target source: (a) as a function of  $\phi$  and (b) as a function of the displacement along the arc of movement defined by the radius  $R + r$  and  $\phi$ . This is approximately  $y$  (see figure A1) when  $\phi$  is small, and shows the relative sensitivity of the cosine source for displacements about the zero position. Thus, in our case  $(R + r)\phi$  was  $\pm 0.5$  mm, in which case  $S$  dropped to  $\approx 0.97$  on either side. See text for details.

ratio  $S$  at the collision region can be determined to first-order by neglecting the spatial extent of the electron beam using the gas beam angular profile  $I(\theta_g)$  as

$$S = \frac{I(\theta_g)/d^2}{I(0)/r^2}, \quad (\text{A.2})$$

where

$$d^2 = (R + r)^2 + R^2 - 2(R + r)R \cos \phi. \quad (\text{A.3})$$

In general, for a tube collimator  $I(\theta_g)$  has a complicated form, but for a cosine source, namely  $I(\theta_g) = I_0 \cos(\theta_g)$ , it is well characterized. Using  $R = 6.7$  mm and  $r = 6$  mm, which are the values of our experimental setup, we get the dependence of  $S$  on  $\phi$  in figure A2. As can be seen, the collimating source only needs to be pivoted by a few degrees in  $\phi$  to obtain a large

change in beam intensity. In this case, the horizon of the tube ( $\theta_g = 90^\circ$ ) is reached when, from equation (A.1),

$$\phi = \cos^{-1} \left[ \frac{R}{R+r} \right], \quad (\text{A.4})$$

which is  $23.4^\circ$  in our setup (see also figure A2(a)). Realistically, including the effect of background gas in the collision region increases the background so that typically the signal + background to background ratio is significantly lower, lying between the extremes of 2:1 (low  $E_0$  and small  $\theta$ ) to 50:1 (high  $E_0$  and large  $\theta$ ) for a  $\phi$  deflection of  $15^\circ$ – $20^\circ$ . As a function of displacement about the collision region (figure A2(b)), we observe that the cosine source is ideal, because it is a broad angular gas distribution source and therefore remarkably insensitive to misalignments of the aperture, in our case by about 3–4%, for the moveable source arrangement.

## References

- [1] Brunger M J and Buckman S J 2002 *Phys. Rep.* **357** 215
- [2] Whelan C T and Mason N J 2005 *Electron Scattering from Atoms, Molecules Nuclei and Bulk Matter* (New York: Kluwer)
- [3] Lister G G, Lawler J E, Lapatovich W P and Godyak V A 2004 *Rev. Mod. Phys.* **76** 541
- [4] Strickland D J, Lean J L, Meier R R, Christensen A B, Paxton L J, Morrison D, Craven J D, Walterscheid R L, Judge D L and McMullin D R 2004 *Geophys. Res. Lett.* **31** L03801
- [5] Boudaïffa B, Cloutier P, Hunting D, Huels M A and Sanche L 2000 *Science* **287** 1658–60
- [6] Tonzani S and Greene C H 2006 *J. Chem. Phys.* **125** 094504
- [7] Winstead C and McKoy V 2006 *J. Chem. Phys.* **125** 074302
- [8] Stangeby P C 2000 *The Plasma Boundary of Magnetic Fusion Devices* (Bristol: Institute of Physics Publishing)
- [9] Srivastava S K, Chutjian A and Trajmar S 1975 *J. Chem. Phys.* **63** 2659
- [10] Trajmar S, Register D F and Chutjian A 1983 *Phys. Rep.* **97** 219
- [11] Nesbet R K 1979 *Phys. Rev. A* **20** 58
- [12] Register D F, Trajmar S and Srivastava S K 1980 *Phys. Rev. A* **21** 1134
- [13] Winstead C and McKoy V 1996 *Adv. At. Mol. Opt. Phys.* **36** 183
- [14] Panajotovic R, Kitajima M, Tanaka H, Jelisavcic M, Lower J, Campbell L, Brunger M J and Buckman S J 2003 *J. Phys. B: At. Mol. Opt. Phys.* **36** 1615
- [15] Brinkmann R T and Trajmar S 1981 *J. Phys. E: Rev. Sci. Instrum.* **14** 245
- [16] Olander D R and Kruger V 1970 *J. Appl. Phys.* **41** 2769
- [17] Rugamas F, Roundy D, Mikaelian G, Vitug G, Rudner M, Shih J, Smith D, Segura J and Khakoo M A 2000 *Meas. Sci. Technol.* **11** 1750
- [18] Ramsey N F 1990 *Molecular Beams* (New York: Oxford University Press) chapter 2
- [19] Winstead C and McKoy B V 2007 private communication
- [20] Khakoo M A, Beckmann C E, Trajmar S and Csanak G 1994 *J. Phys. B: At. Mol. Opt. Phys.* **27** 3159
- [21] Hughes M, James K E Jr, Childers J G and Khakoo M A 2003 *Meas. Sci. Technol.* **14** 841
- [22] Schow E, Hazlett K, Medina C, Vitug G, Childers J, Bray I and Khakoo M A 2005 *Phys. Rev. A* **72** 062717
- [23] Childers J, James K, Hughes M, Bray I, Baertschy M, Kanik I and Khakoo M A 2004 *Phys. Rev. A* **69** 022709
- [24] Khakoo M A, Jayaweera T, Wang S and Trajmar S 1993 *J. Phys. B: At. Mol. Opt. Phys.* **26** 4845
- [25] Sagara T and Boesten L 1998 *J. Phys. B: At. Mol. Opt. Phys.* **31** 3455
- [26] Shyn T W and Carignan G R 1980 *Phys. Rev. A* **22** 923
- [27] Nickel J C, Mott C, Kanik I and McCollum D C 1988 *J. Phys. B: At. Mol. Opt. Phys.* **21** 1867
- [28] Gote M and Ehrhardt H 1995 *J. Phys. B: At. Mol. Opt. Phys.* **28** 3957
- [29] Bouchiha D, Gorfinkel J D, Caron L G and Sanche L 2007 *J. Phys. B: At. Mol. Opt. Phys.* **40** 1259